34th Annual International Conference of the IEEE EMBS
San Diego, California USA, 28 August - 1 September, 2012

An influence of spontaneous spike rates on information transmission in a spherical bushy neuron model with stochastic ion channels

Hiroki Arata, *Student Member IEEE*, and Hiroyuki Mino, *Senior Member IEEE*

***Abstract*— This article presents an effect of spontaneous spike firing rates on information transmission of the spike trains in a spherical bushy neuron model of antero-ventral cochlear nuclei. In computer simulations, the synaptic current stimuli ascending from auditory nerve fibers (ANFs) were modeled by a filtered inhomogeneous Poisson process modulated with sinusoidal functions, while the stochastic sodium and stochastic high- and low-threshold potassium channels were incorporated into a single compartment model of the soma in spherical bushy neurons. The information rates were estimated from the entropies of the inter-spike intervals of the spike trains to quantitatively evaluate information transmission in the spherical busy neuron model. The results show that the information rates increased, reached a maximum, and then decreased as the rate of spontaneous spikes from the ANFs increased, implying a resonance phenomenon dependent on the rate of spontaneous spikes from ANFs. In conclusion, this phenomenon similar to the stochastic resonance would be observed due to that spontaneous random spike firings coming from auditory nerves may act as an origin of fluctuation or noise, and these findings may play a key role in the design of better auditory prostheses.**

***Index Terms*— Stochastic Hodgkin-Huxley model, Antero-ventral cochlear nucleus, Spherical bushy cell, Spontaneous spike rate**

I. INTRODUCTION

Cochlear nuclei have been considered as the second-order neuron of the auditory nervous system in relaying sound stimuli from the primary auditory nerve to the superior olive complex (SOC) working for sound localization. The spherical bushy neuron of cochlear nuclei has been reported to preserve temporal information with a greater precision for detecting interaural time differences (ITD) in medial superior olive (MSO) of the SOC [1], [2]. For a greater temporal precision, spherical bushy neuron receives a supra-threshold stimulus coming from a couple of ANFs onto the soma with a special morphology of synapses, i.e., the form of an endbulb of Held. Moreover, the spherical bushy neurons have not only high-threshold potassium channels, but a different kind of potassium channels, i.e., low-threshold potassium channels, to sharpen the waveform of action potentials [3].

Nevertheless, a high level of spontaneous spike firing activity with random fashion has been observed in auditory brainstem nuclei even in the absence of a sound stimulus [4], [5]. Liberman has suggested that fibers with different spontaneous rates have different ascending projections in the cochlear nuclei [6], [7]. However, it has been unclear how come spontaneous random activity was observed in the cochlear nuclei relaying sound stimuli to the MSO detecting ITD with a microsecond temporal precision.

H. Arata is with Graduate School of Engineering, Kanto Gakuin University, 1-50-1, Mutsuura E., Kanazawa-ku Yokohama 236-8501, Japan hi.arata.0214@gmail.com, H. Mino is with Department of Electrical and Computer Engineering, Kanto Gakuin University, 1-50-1 Mutsuura E., Kanazawa-ku, Yokohama 236-8501, Japan mino@ieee.org

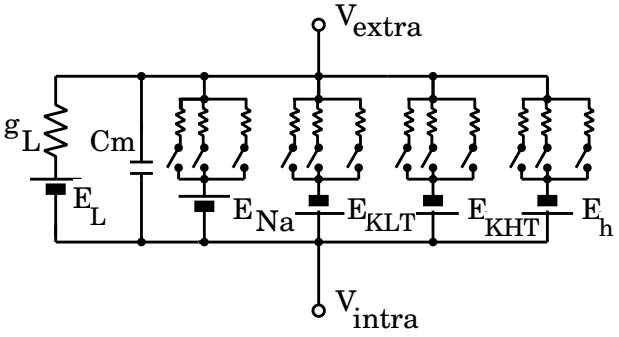

Fig. 1. Electrical equivalent circuit of a spherical bushy neuron model with four kinds of stochastic ion channels.

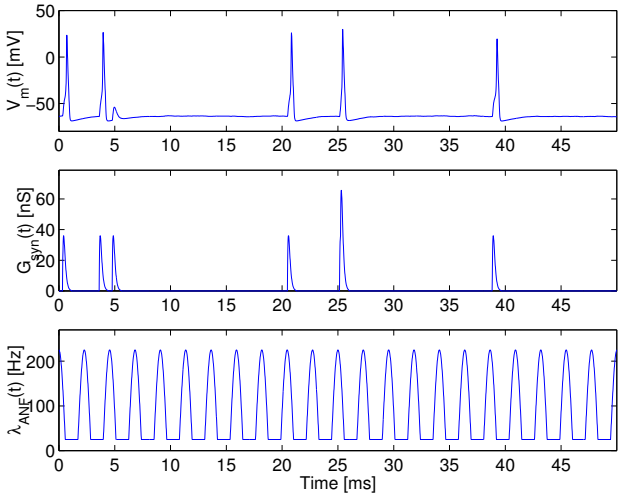

Fig. 2. An illustrative example of a membrane potential (top), an excitatory synaptic conductance with an alpha function (middle), an intensity function of the inhomogeneous Poisson process modulated by a sinusoidal function (bottom) as a function of time.

The objective of this article was to investigate an influence of spontaneous spike firing rates on information transmission of the spike trains in a spherical bushy neuron model of the antero-ventral cochlear nucleus, from an information-theoretic point of view, through computer simulations.

II. METHODS

A soma of spherical bushy neurons was represented by a single-compartment model in which the diameter of

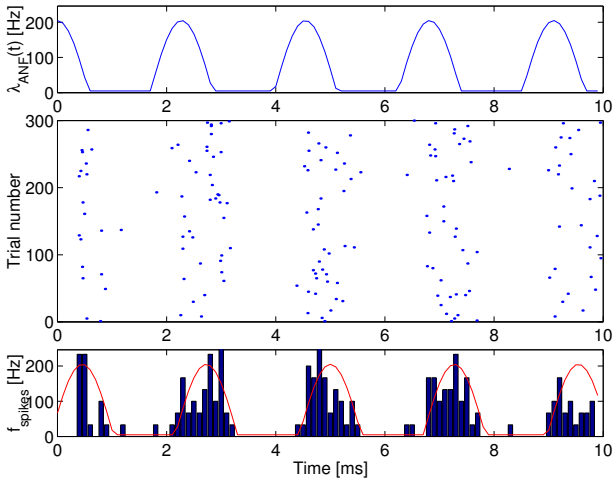

Fig. 3. An intensity function (top), raster plots (middle), the estimated spike firing rates (bottom) as a function of time at λ_{spon}=$5s^{-1}$.

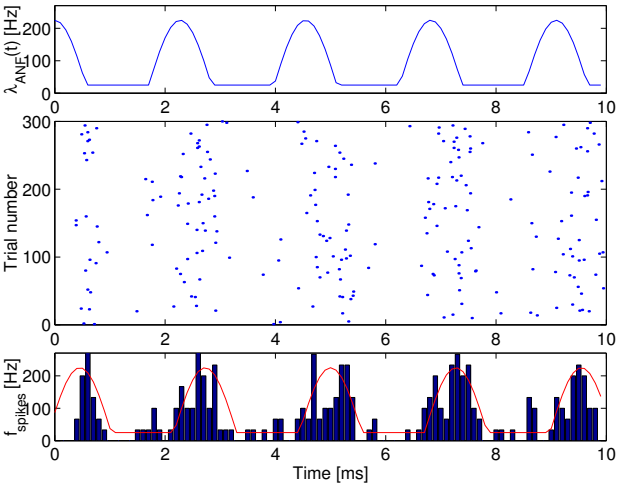

Fig. 4. An intensity function (top), raster plots (middle), the estimated spike firing rates (bottom) as a function of time at λ_{spon}=$25s^{-1}$.

the soma, d, was set at $21\mu m$, and the capacity of cell membranes was $0.9\mu F/cm^2$. The modified Hodgkin-Huxley model consisted of four types of ion channels of sodium channels(Na) and high- and low-threshold potassium channels(KHT,KLT) and cation channels(h) with stochastic ion channel models. The electrical equivalent circuit of the neuron model is shown Figure 1. According to Kirchhoff's current law, the transmembrane potentials, $V_m(t)$, can be expressed as a function of time as follows :

$$C_m\frac{dV_m(t)}{dt}+2(I_{Na}(t)+I_{KLT}(t)+I_{KHT}(t) +I_h(t)+I_L)=I_{ANF}(t) \quad (1)$$

in which a scaling factor of 2 was adopted according to the literature [9], and the resting potential, E_{rest}, was set at -65

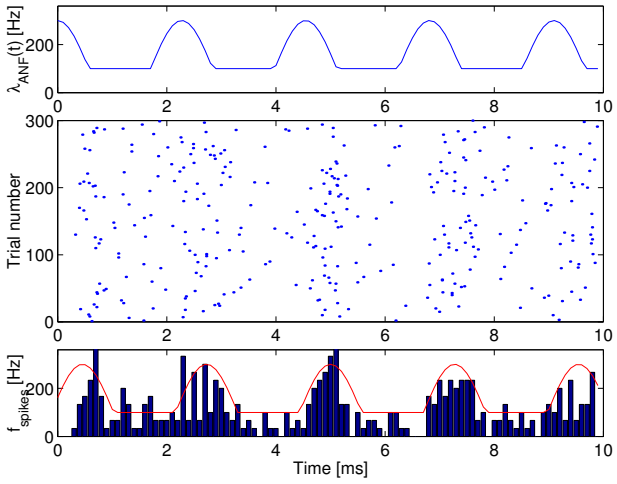

Fig. 5. An intensity function (top), raster plots (middle), the estimated spike firing rates (bottom) as a function of time at λ_{spon}=$100s^{-1}$.

mV, and where

$$\begin{aligned} I_{Na}(t)&=\gamma_{Na}N_{Na}(t)(V-E_{Na})\\ I_{KLT}(t)&=\gamma_{KLT}N_{KLT}(t)(V-E_K)\\ I_{KHT}(t)&=\gamma_{KHT}[0.85N_n(t)+0.15N_p(t)](V-E_K)\\ I_h(t)&=\gamma_hN_h(t)(V-E_h)\\ I_L&=\bar{g}_L(V-E_L) \end{aligned} \quad (2)$$

in which $Nx(t)'s$ stand for the number of open channels in each ion channel ($x=Na,KLT,n,p,h$). Each ion channel followed the discrete-state Markov processes with eight states for sodium channels, ten states for low-threshold potassium channels, three states for high-threshold potassium channels, two states for high-threshold potassium channels, and two states for cation channels. These were implemented by the Channel Number Tracking algorithm [8]. The state transition rate was multiplied by a values of $1/0.17$ so that the temperature can be set at 38 C according to the literature [3], where E_{Na}=$55mV$, E_K=-$70mV$, E_h=-$43mV$, and E_L=-$65mV$. The single conductance was expressed as follows :

$$\begin{aligned} \gamma_{Na}&=\bar{g}_{Na}/N_{Na}^{max} & N_{Na}^{max}&=6S_{soma}\\ \gamma_{KLT}&=\bar{g}_{KLT}/N_{KLT}^{max} & N_{KLT}^{max}&=2S_{soma}\\ \gamma_{KHT}&=\bar{g}_{KHT}/N_{KHT}^{max} & N_{KHT}^{max}&=2S_{soma}\\ \gamma_h&=\bar{g}_h/N_h^{max} & N_h^{max}&=2S_{soma} \end{aligned} \quad (3)$$

where the parameters were set as follows : $S_{soma}=4\ \pi(d/2)^2$, $\bar{g}_{Na}$=$3.03\times1000\ nS$, $\bar{g}_{KLT}$=$3.03\times200\ nS$, $\bar{g}_{KHT}$=$3.03\times150\ nS$, $\bar{g}_h$=$3.03\times20\ nS$, $\bar{g}_L$=$3.03\times2\ nS$.

The excitatory synaptic current $I_{ANF}(t)$ ascending from the primary auditory nerve fiber was modeled as a filtered inhomogeneous Poisson process :

$$I_{ANF}(t)=\int_{-\infty}^{t}G_{syn}(t-\tau)(V_m(t)-E_e)dN_{ANF}(\tau) \quad (4)$$

where the equilibrium potential of excitatory synapses was set at E_e=$0mV$, and the synapse conductance waveform was the alpha function expressed as :

$$G_{syn}(t)=\bar{g}_e\frac{t}{\tau_e}exp[1-\frac{t}{\tau_e}] \quad (5)$$

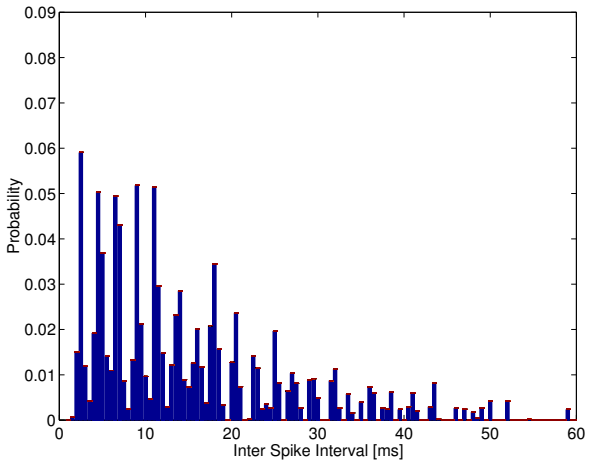

Fig. 6. Inter-Spike Interval Histogram at $\lambda_{spon} = 5s^{-1}$.

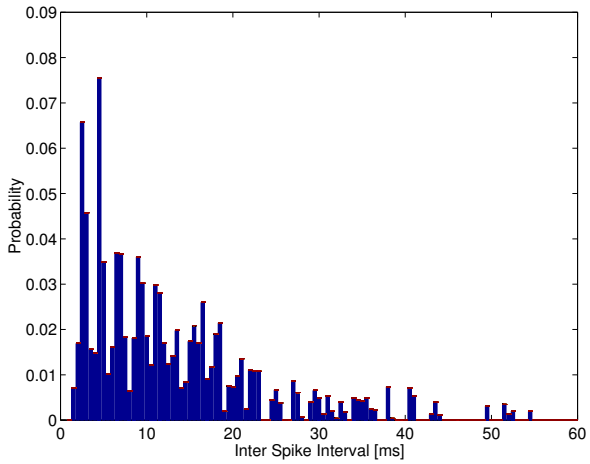

Fig. 7. Inter-Spike Interval Histogram at $\lambda_{spon} = 25s^{-1}$.

where the maximum of excitatory synaptic conductance was set at g_e=36nS, the time constant was set at τ_e=0.1ms, the excitatory synaptic equilibrium potential was set at E_e=0mV. The conductance was set such that the current stimulus could be always a supra-threshold stimulus ; that is, the Firing Efficiency(FE), defined by the number of spike firings divided by the number of stimulus presentations, could become 1.0 because of a specific morphology of synaptic structure, i.e., an endbulb of Held.

$N_{ANF}(t)$'s denote the counting process of an inhomogeneous Poisson process, described by the following intensity function :

$$\lambda_{ANF}(t) = \lambda_{spon} + \tilde{\lambda}_{sinusoid}(t) \tag{6}$$

where the intensity function is modulated by the sinusoidal function :

$$\tilde{\lambda}_{sinusoid}(t) = \begin{cases} \lambda_c cos(2\pi ft) & (\tilde{\lambda}_{sinusoid}(t) > 0) \\ 0 & (otherwise) \end{cases} \tag{7}$$

where $f = 440Hz$, and $\lambda_c = 200s^{-1}$. In order to investigate a dependency of spontaneous firing rates, λ_{spon} was varied as 5, 25, 50,75,100, and $125s^{-1}$.

In computer simulations, (1) was solved in terms of $V_m(t)$'s with the Runge-Kutta method and the inter-spike intervals, T, were calculated from the spike trains to estimate the information rate $I_{rate}bits/s$ as follows :

$$I_{rate}(I_{ANF}(t), T) = R[H_{total}(T) - H_{noise}(T|I_{ANF}(t))] \tag{8}$$

where the total entropy is expressed as :

$$H_{total}(T) = -\sum_{i=0}^{\infty} p(T_i) log_2 p(T_i) \tag{9}$$

and the noise entropy is expressed as :

$$H_{noise}(T|I_{ANF}(t)) = -E[\sum_{i=0}^{\infty} p(T_i|I_{ANF}(t)) log_2 p(T_i|I_{ANF}(t))] \tag{10}$$

where R denotes the spike firing rate, and $E[\,]$ designates the expection operation.

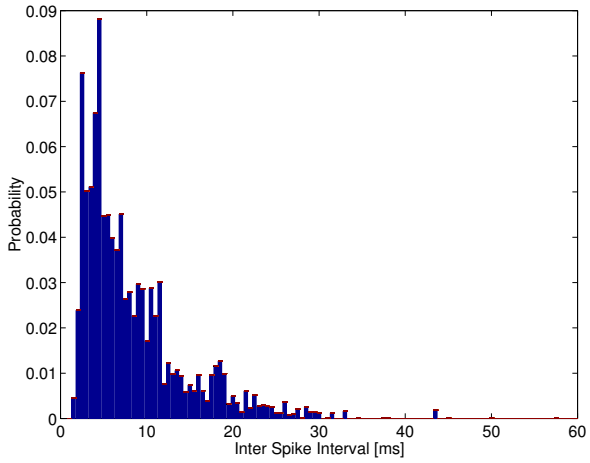

Fig. 8. Inter-Spike Interval Histogram at $\lambda_{spon} = 100s^{-1}$.

III. RESULTS

The transmembrane potential, the conductance of the excitatory synapse, and the intensity function of an inhomogeneous Poisson process are depicted as a function of time in Figure 2, when the synaptic conductance is set such that the expectation can become the supra-threshold, i.e., FE=1.0, except for a refractory period.

Figure 3 shows an intensity function (top), raster plots of 300 realizations (middle), the post-stimulus time histogram (PSTH) as the estimated spike firing rates superimposed on the genuine value of the intensity function (bottom) as a function of time for 10 ms in time length at λ_{spon} = 5 s^{-1}. The PSTH's were generated with a bin width of 0.1 ms in the bottom of Figure 3. It follows from the traces that the spike firing rate is not necessarily encoded to sinusoidal functions at a frequency of 440 Hz.

The intensity function (top), raster plots of 300 realizations (middle), the post-stimulus time histogram (PSTH) are depicted in Figure 4 in the case of λ_{spon} = 25 s^{-1} at a frequency of 440 Hz. It can be seen that the spike firing rates estimated are a good agreement with a sinusoidal

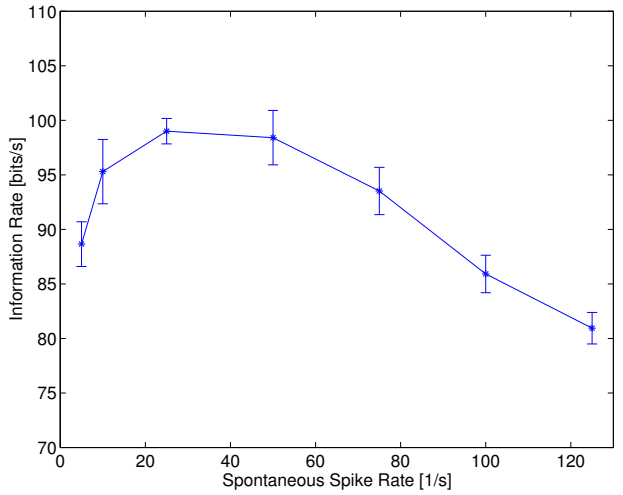

Fig. 9. Information rate as a function of spontaneous spike firing rate.

component of the intensity function at a frequency of 440 Hz, i.e., an implication being encoded well with the sinusoidal information into the spike trains.

Figure 5 also shows the intensity function (top), raster plots of 300 realizations (middle), the PSTH at λ_{spon} = 100 s^{-1} at a frequency of 440 Hz. However, an encoding property of sinusoidal functions was not good enough due to a greater rates of spontaneous spike activities in a poor synchronization to the sinusoidal function at a frequency of 440 Hz.

Although the raster plot and PSTH could give us an insight into a dependency of the spontaneous rates on sinusoidal encoding, they would only provide us with a qualitative impression. Instead, we adopted to evaluate quantitatively the information rates of the spike trains in response to the synaptic currents, driven by the primary auditory nerve.

The information rates were estimated by multiplying the mutual information to the spike firing rates according to (6) in which the mutual information was estimated from observations of the ISI histograms, as the spontaneous rates, λ_{spon}, were varied to 5, 25, 50, 75, 100, and 125s^{-1}. Figures 6-8 show the ISI histograms used in estimating the total entropy, when the spontaneous rate, λ_{spon}, was set at 5, 25, and 100 s^{-1}.

The information rates calculated on the basis of (8), (9) and (10) as a function of the spontaneous rate λ_{spon} are depicted in Figure 9. The information rate increased, reached a maximum, and then decreased as the spontaneous rate was increased, like a typical curve of the stochastic resonance. As a result, a resonance phenomenon was observed as a function of the spontaneous spike rates of the ANFs.

IV. CONCLUDING REMARKS

In this article, we have investigated how the spontaneous spike firing rates, λ_{spon}, affected information transmission of the spherical bushy neuron model in the case of supra-threshold synaptic current stimuli due to an endbulb of Held. In the computer simulations, the resonance phenomena of the information rates as a function of λ_{spon} were observed, like a supra-threshold stochastic resonance (SSR) [11], [12], [13], [14] as a function of the intensity of extrinsic fluctuations. However, the characteristics of this resonance phenomenon would not be essentially different from those of the regular SSR observed in a population of neurons. The reasons are two folds : (i) the spherical bushy neuron model used in this study was assumed to be just a single neuron, not a population of neurons, (ii) any extrinsic noise was not applied to the spherical bushy neuron model. It is suggested that a combination of the spontaneous random spike firings with the intrinsic fluctuations due to stochastic ion channels makes it possible to create this resonance phenomenon, without applying an extrinsic noise. In conclusion, a specific rate of the spontaneous spike firings may play an important role in information transmission of the spike trains in the spherical bushy neuron relaying precisely temporal information on the primary auditory nerve to the SOC. These findings may advance our understanding of information transmission in spherical bushy neurons and may accelerate the design of better auditory prosthesis in auditory brainstem implants (ABI) [15].

REFERENCES

[1] J. Blauert, ***Spatial Hearing : The Psychophysics of Human Sound Localization***, The MIT Press, Cambridge, 1997.

[2] E. Kandel, J. Schwartz, and T. Jessell, ***Principles of Neural Science***, Fourth Editin, McGraw-Hill Medical, New York, 2000.

[3] J. S. Rothman and P. B. Manis, "The Roles Potassium Currents Play in Regulating the Electrical Activity of Ventral Cochlear Nucleus Neurons," ***J. Neurohysiol.***, Vol.89, pp.3097-3113, 2003.

[4] L. C. Liberman, "Auditory-nerve response from cats raised in a low-noise chamber," ***J. Acoust. Soc. Am.***, 63, pp.442-455, 1978.

[5] L. C. Liberman, "Single-neuron labeling in the cat auditory nerve," ***Science***, 216, pp.1239-1241, 1982.

[6] L. C. Liberman, "Central projections of auditory-nerve fibers of different spontaneous rate I. Anteroventral cochlear nucleus," ***J. Comp Neurol.***, 313, pp.240-258, 1991.

[7] L. C. Liberman, "Central projections of auditory-nerve fibers of different spontaneous rate II. Posteroventral and dorsal cochlear nuclei," ***J. Comp Neurol.***, 327, pp.17-36, 1993.

[8] H. Mino, J. T. Rubinstein, and J. A. White, "Comparison of Algorithms for the Simulation of Action Potentials with Stochastic Sodium Channels," ***Ann. Biomed. Eng.***, Vol. 30, pp. 578-587, 2002.

[9] Y. Gai, B. Doiron, V. Kotak, and J. Rinzel, "Noise-Gated Encording of Slow Inputs by Auditory Brain Stem Neuron With a Low-Threshold K+ Current," ***J. Neurohysiol.***, Vol.102, pp.3447-3460, 2009.

[10] A. Zador, "Impact of synaptic unreliability on the information transmitted by spiking neurons," ***J. Neurophysiol.***, Vol. 79, pp.1219-1229, 1998.

[11] N. G. Stocks, "Suprathreshold Stochastic Resonance in Multilevel Threshold Systems," ***Phys. Rev. Letters***, Vol. 84, pp.2310-2313, 2000.

[12] N. G. Stocks, "Information transmission in parallel threshold arrays : Suprathreshold stochastic resonance," ***Phys. Rev. E***, Vol. 63, Art. No. 041114, 2001.

[13] N. G. Stocks and R. Mannella, "Generic noise enhanced coding in neuronal arrays," ***Phys. Rev. E***, Vol. 64, Art. No. 030902(R), 2001.

[14] T. Hoch, G. Wenning and K. Obermayer, "Optimal noise-aided signal transmission through populations of neurons," ***Phys. Rev. E***, Vol. 68, Art. No. 011911, 2003.

[15] V. Colletti and R. V. Shannon, "Open Set Speech Perception with Auditory Brainstem Implant ?," ***The Laryngoscope***, Vol. 115, pp. 1974-1978, 2005.